Int. J. Electrochem. Sci., 16 **(2021)** Article ID: 210936, doi: 10.20964/2021.09.05

International Journal of
ELECTROCHEMICAL
SCIENCE
www.electrochemsci.org

The Cathodic Reduction of Zn（Ⅱ）on the Zn and Au Electrode in the Zinc(Ⅱ)–NH_4Cl System

Qingfeng Shen[1], Shuangquan Xu[1], Wenzhi Zhang[1], Xiaohua Yu[1,], Chunxia Liu[2,*]*

[1] Faculty of Metallurgical and Energy Engineering, Kunming University of Science and Technology, Kunming, 650093, PR China;
[2] Analyses and Test Research Center, Kunming University of Science and Technology, Kunming, 650093, PR China;
[*]E-mail: yxhyxh1978@ailun.com, cxliu1976@sina.com

Received: 8 September 2020 / *Accepted:* 18 January 2021 / *Published:* 10 August 2021

In recent years, the leaching of complex minerals containing zinc using the ammonia method has attracted much attention, but there are few basic studies of the cathodic reduction in the zinc(Ⅱ)–NH_4Cl system. In this paper, the differences of Zn (II) reduction on the gold electrode and the zinc electrode were compared using cyclic voltammetry (CV), and the factors of influencing Zn(II) reduction on the zinc electrode were investigated by using a steady-state polarization curve method. The influence of temperature and the potential scope on the hydrogen evolution reaction was investigated using linear potential sweep and chronocoulometry on the zinc electrode. The results show that the discharge velocity of Zn (II) on the zinc electrode was faster than on the gold electrode, and the change from steady-state to transient Zn (II) on the zinc electrode was easily affected by the scanning rate. This is an effective method of increasing the temperature, intensity of stirring and Zn (II) concentration to Zn (II) reduction due to the depolarization effect. The form of Zn (II) was related to the NH_4^+ concentration in the solution. Increasing NH_4^+ concentration played a polarization role on Zn (II) deposition. The electron transfer coefficient of the hydrogen-evolution reaction was in direct proportion to temperature in the electrodeposition process, and the hydrogen evolution reaction was aggravated with an increase in the cathode overpotential.

Keywords: Zinc(Ⅱ)–NH_4Cl system; Zinc electrodeposition; cathodic reduction; Substrate

1. INTRODUCTION

The traditional process of electrolyzing zinc in a sulfuric acid system has been used by industry for many years, but a great deal of practice has shown that this technology has many shortcomings: for example, its energy consumption is high, there is difficulty in achieving the requirements for liquid

electrolytic purification (time for desilication products to settle out, iron purification process, presence of fluorine, chlorine and other complexes), there is difficulty in removing fluoride and chloride (F^- and Cl^- accumulate in the circulating electrolyte, causing corrosion of the cathode and anode, difficulty in stripping the zinc, and a lower grade of zinc). With resources of zinc sulfide concentrate becoming scarce, it has become necessary to expand sources of zinc-containing raw materials, and more and more workers in the theoretical study of science and technology are seeking to replace the electrolytic zinc sulfuric acid system, in order to make efficient use of low-grade ores of zinc oxide and hot galvanizing slag, etc. containing zinc [1,2].

Nowadays, hydrometallurgy in ammonium chloride solution is considered to be a prospective medium for extracting nonferrous metals [3,4]. The reason probably lies in the ammonia salt method which can selectively leach copper, zinc, cobalt, nickel and other valuable metals [5-10]. Ammonia salt has almost no reaction with Fe_2O_3, SiO_2, CaO or MgO, producing a pure leaching solution. It has already been applied to the recovery of other low-grade ores of copper, nickel, cobalt, etc. and to secondary resources, but it is still in the research stage in zinc hydrometallurgy.

Some researcher [11-14] explored the dissolution thermodynamics, anodic reaction kinetics, electrolysis technology and other aspects of using low-grade zinc oxide ore, zinc dust, zinc slag and other complex materials containing zinc in a Zn(II)–NH_3.H_2O–NH_4Cl system. However, few basic studies of the Zn^{2+} cathode reduction in a Zn(II)–NH_4Cl system have been reported [15], The study adopts the zinc bar as a working electrode, of course, studying zinc electro deposition mechanism also can use other electrode, such as Ti, Glassy carbon and 316 L in the system of ammonium chloride[16]. Considering the surface of the cathode is covered with a layer of zinc in a relatively short period, studying Zn^{2+} reduction behavior on zinc electrode is closer to the actual production situation. But cyclic voltammetry method will cause the zinc electrode oxidization dissolution. Therefore, Zn and Au electrode were used for studying cathode reduction behavior of Zn（Ⅱ）in the zinc(Ⅱ)–NH_4Cl system.

2. EXPERIMENTAL DETAILS

2.1. Testing system

The electrolyte solutions were prepared using distilled water and metal salts of analytical grade (XiLong Chemical Co., Ltd., China). The electrolyte solutions were prepared with 60 g/l Zn^{2+} ($ZnCl_2$) and 40 g/l NH_4^+ (NH_4Cl). The electrolytic temperature was controlled by a constant temperature magnetic stirring apparatus.

The experiments were carried out using an electrochemical workstation (AutlabPGSTAT204), produced by Metrohm AG.

The experiments were conducted in a 100 ml electrolytic cell. A three-electrode set-up comprised: a 1 cm^2 double platinum sheet as an auxiliary electrode, the saturated calomel electrode (SCE) as the reference electrode (RE), and a zinc electrode and a gold electrode as the working electrodes, respectively, the working electrodes were L type and ϕ = 3 mm (0.070686 cm^2). All potentials were referred to the SCE and were not corrected for ohmic drop.

2.2. Measurements methods

Before each measurement, the working electrode was sequentially polished to a mirror surface using metallographic sandpapers No.s 4 and 5 and 0.05 μm Al_2O_3 powder. Then the working electrode and the auxiliary electrode were washed with distilled water. When it was ready to test, the working electrode was soaked in a solution for 3 min to stabilize the open circuit potential (OCP). In addition to the experiment of 3.2.2 part adopted stirring, other experiments had not been stirred, and the whole experiment process in airtight electrolytic cell.

Cyclic voltammetry (CV) curves comparing the gold electrode and the zinc electrode were obtained using scan rates from 5 mV/s to 300 mV/s. The OCP was measured before the scan, scanning began with OCP to more negative direction, swept back to near the OCP potential. The scanning rate of the steady linear sweep voltammetry (LSV) curves on the zinc electrode was 1 mV/s, the start potential was OCP, and the termination potential was −1.4 V. When investigating the influence of the electrolyte temperature on the hydrogen evolution reaction, potassium chloride was used to replace the zinc chloride electrolyte in order to shield the reaction on the electrode from Zn^{2+} interference, the other conditions remaining unchanged. The influence of electrode potential on H^+ reduction was studied with the gold electrode as the working electrode. A chronocoulometry curve was obtained using a scanning rate of 200 mV/s.

3. RESULTS AND DISCUSSION

3.1. Cyclic voltammetry investigation of both substrates

Fig. 1 shows the cycle voltammogram obtained from zinc (Ⅱ) – NH_4Cl electrolyte on the gold electrode (the potential range of -0.4V to -1.6V). Fig. 2 shows the cycle voltammogram on the zinc electrode (the potential range of -0.9V to -1.7V). A comparison to Figs 1 and 2: the peak potentials (φ_p) of Zn^{2+} reduction were substantially in the same position on both electrodes, and $|\varphi_p|$ increased with the scanning rate increasing, this shows that Zn^{2+} reduction reactions were irreversible on both electrodes. But the total current ($|j|$) of the Zn^{2+} reduction on the gold electrode was lower than that on the zinc electrode at the same scanning rate and control potential, which indicates that Zn^{2+} or H^+ was reduced more easily on the zinc electrode. Furthermore, when the scanning rate was small, it can be seen that the change in the Zn^{2+} current value was smaller on the zinc electrode than on the gold electrode when scanning through different time periods at the same potential. When the scanning rate was higher, the opposite was found, which indicates that Zn^{2+} reduction tended to be steadier on the zinc electrode at a low scan rate, and the Zn^{2+} change from a steady to a transient state on the zinc electrode was easily affected by scan rate. Electrochemistry analysis of the zinc electrodeposition in NH_4Cl – NH_3 electrolytes on Ti, Glassy Carbon and 316L Stainless Steel have been studied by Jorge et al.[16] The onset of the zinc deposition depended on the cathode material, the surface of 316L Stainless Steel electrode exhibited the smallest overpotential, followed by the Glassy Carbon and Ti surfaces.

Fig. 2 shows that the current increased rapidly and then declined at the beginning of the scan. These changes were due to electric double layer charging. As potential shifted toward negative, a fast increase in cathodic current density was observed, resulting in peak current corresponding to the reduction of the Zn^{2+}. The potential continue to shift negatively, the reduction current decreased gradually and stabilize to the level value close to the scanning reversing potential φ_λ. After φ_λ, the scanning turned to the opposite direction, and formed the negative current. When the scanning rate was 5mV/s, the current peak had difficulty forming, and the scan positive current coincided mainly with the negative current at the same potential, which was close to a steady state. Therefore, it was suggested that scanning rate was less than 5mV/s when steady state polarization curve was tested.

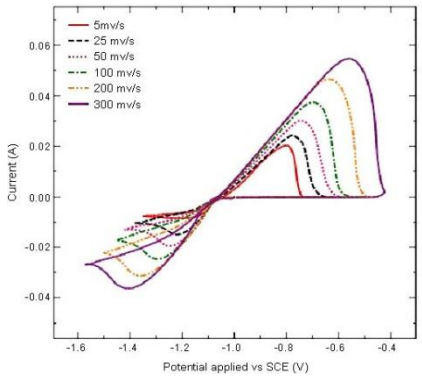

Figure 1. The cycle voltammetry curves of Zn^{2+} on the gold electrode in zinc (Ⅱ) – NH_4Cl electrolyte at different scanning speeds (the potential range of -0.4V to -1.6V)

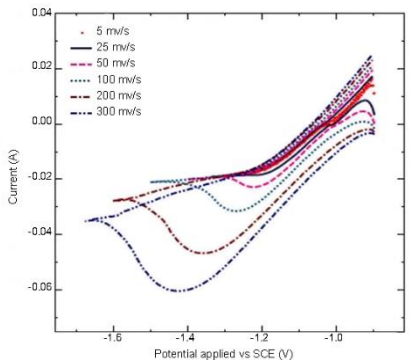

Figure 2. The cycle voltammetry curves of Zn^{2+} on the zinc electrode in zinc (Ⅱ) – NH_4Cl electrolyte at different scanning speeds (the potential range of -0.9V to -1.7V)

Table 1 shows some voltammetric behavior results counting from Fig. 2. It shows that the reduction peak current increased with the scan rate increasing, the reduction current peak height i^p was proportional to a scan rate of $V^{1/2}$ at different scanning rates. This proves that Zn^{2+} reduction reaction was an irreversible electrode reaction process again, and the degree of irreversibility increased with the scanning rate increasing. Ma et al.[15] also found that the Zn^{2+}reduction reaction in $ZnCl_2$ – NH_4Cl solution is irreversible electrode process, and has the dynamic law of two charge transfer one step completion and charge transfer control.

According to the relationship between irreversible electrode reactions [$\varphi_p - \varphi_{p/2} = (48.5/\alpha n)$ mV (30°C)] and the value of $\varphi_p - \varphi_{p/2}$ from Table 1, αn could be obtained as 0.605, 0.575, 0.506, 0.396, 0.334 at scan rates of 25 ~ 300 mV/s, respectively. This indicates that the electron transfer number n = 1 of controlling step in the Zn^{2+} deposition process, and the electron transfer coefficients α were 0.605, 0.575, 0.506, 0.396, 0.334 respectively. This combined to Fig. 2 peak shape, it shows that the reduction of Zn^{2+} was a two-electron tandem reaction, and the control step was the first step (because Zn^{+} is more unstable than Zn^{2+} and Zn). The electron transfer coefficients α gradually decreased as the scan potential rate accelerated, because the Zn^{2+} deposition was different at different potential change rates on the zinc electrode, and the zinc electrode surface changed to a different surface structure with the progress of gradual Zn^{2+} electrodeposition. Because $i^p \propto V^{1/2}$ and because of the relationship of αn with potential scan rate, the total mass transfer coefficient D_O of the electrode reaction increased with an increase in the potential scan rate, which was due to D_O being affected comprehensively by electromigration, mass transfer by diffusion, and mass transfer by convection.

Table 1. The parameter list for half-cycle voltammetry curves of Zn^{2+} on the zinc electrode

Scan rate (mV/s)	Peak position (V)	Peak height (A)	Peak area $Q(C)$	$\varphi_p - \varphi_{p/2}$ （mV）	Peak width half-height （V）
5	–	–	–	–	–
25	−1.166	−0.0071	−0.0246	80.2	0.180
50	−1.197	−0.0124	−0.0367	84.4	0.191
100	−1.252	−0.0197	−0.0455	95.9	0.238
200	−1.338	−0.0288	−0.0484	122.4	0.319
300	−1.398	−0.0364	−0.0548	145.1	0.379

3.2. Study of influence factors on Zn^{2+} reduction

3.2.1. Effect of electrolyte temperature

Fig. 3a shows LSV curves of Zn^{2+} reduction on the zinc electrode in zinc (Ⅱ) – NH_4Cl electrolyte at different temperatures (the potential range of -1.0V to -1.4V). As can be seen from Fig. 3a, in the early Zn^{2+}deposition, the deposition reaction rate had little difference at different temperatures, because the Zn^{2+} concentration on the electrode surface was the same, and the main factor having an impact on Zn^{2+} polarization in the cathodic reaction was the overpotential, in the early electro deposition. At this time, the electrode reaction was controlled by electrochemical reaction. The Zn^{2+} concentration of the electrode surface reduced as the cathodic reaction continued to conduct. But In the high temperature electrolyte, the reducing was relatively slow. Because the Zn^{2+} transport speed was relatively fast and the mass diffusion coefficient was large, and the Zn^{2+} concentration of the electrode surface could gain a better complement. The electrode reaction entered into the mixing control phase at this moment, electrochemical reaction was dominant. The potential continue to shift negatively, the Zn^{2+} concentration of the electrode surface showed a more significant change with a change in temperature.

The effect of overpotential on the Zn^{2+} cathodic polarization had become less obvious. The electrode reaction was still the mix control phase, and the mass transfer step was the main one. Therefore, the temperature change improved the velocity of ion migration, the mass diffusion coefficient, and the discharge rate of Zn^{2+} on the cathode.

Fig. 3b shows the $\eta_k - \lg i_K$ curves of Zn^{2+} reduction on the zinc electrode in zinc (Ⅱ) – NH_4Cl electrolyte at different temperatures. As can be seen from Fig 3b, with an increase of electrolyte temperature, the OCP of Zn^{2+} on the zinc electrode gradually became negative, and Zn^{2+} had become more active.

For an irreversible electrode reaction, when $i >> i_0$, the relationship between the polarization overpotential and the current density generally obeys the Tafel equation. The Tafel equation can be modified to:

$$\lg i_K = \lg i_0 + n\alpha F \mid \eta_k \mid / 2.303\, RT \qquad (2)$$

From Fig. 3b and equation (2), at electrolyte temperatures of 333.15K and 323.15K, αn were 0.302 and 0.238, respectively, whereas at low electrolyte temperature, αn had smaller values. It is debateable, whether the relationship between potential and current density was an elaboration of the Tafel relationship. There could be two reasons for this: (1) the electrode process was influenced by electrochemical polarization, concentration polarization, and various other factors. The Tafel region of the electrode process was not constant or less obvious, and the electrode process cannot simply be expressed by the Tafel relationship. (2) The partial region between polarization overpotential and current density accorded with a linear relationship, but the coefficients may have other physical and chemical significance. This paper studied the electrochemical mechanism of the influence of temperature on the zinc electrodeposition in the Zn(Ⅱ) – NH_4Cl system, and Wang [17] Only stuided the influence of temperature on the cell voltage and current efficiency of the zinc electrodeposition process, Ma[16] only gave the activation energy of the zinc evolution reaction as 49.2 kJ/mol.

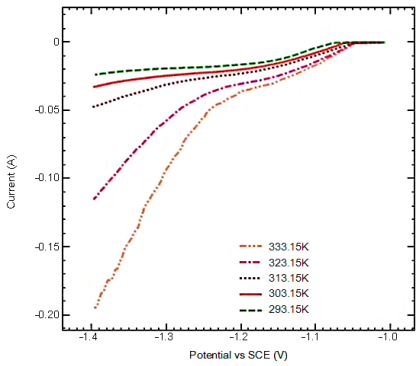

Figure 3.a LSV curves of Zn^{2+} reduction on the zinc electrode in zinc (Ⅱ) – NH_4Cl electrolyte at different temperatures (the potential range of -1.0V to -1.4V)

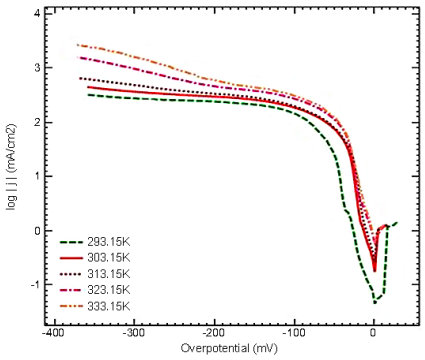

Figure 3.b η_k–lg i_K curves of Zn^{2+} reduction on the zinc electrode in zinc (Ⅱ) – NH_4Cl electrolyte at different temperatures

3.2.2. Effect of stirring intensity

Fig. 4a shows the LSV curves of the Zn^{2+} reduction on the zinc electrode in zinc (Ⅱ) – NH_4Cl electrolyte at different stirring speeds. Fig. 4a shows that a proper stirring intensity helped Zn^{2+} reduction, and the effect was not obvious when the stirring speed was more than a certain degree. This may be because there was diffusion layer between the electrolyte and the electrode. Proper stirring significantly reduced the thickness of the diffusion layer, and increased the mass transfer of the Zn^{2+} from the electrolyte to the electrode surface, but the diffusion layer thickness would not infinitely decrease with constantly increasing of the stirring intensity, so the effect eventually changed little.

Fig. 4b shows the η_k–lgi_K curves of the Zn^{2+} reduction on the zinc electrode in zinc (Ⅱ) – NH_4Cl electrolyte at different stirring speeds. Fig. 4b shows that the OCP of Zn^{2+} on the zinc electrode had a slight positive deflection with an increase of the stirring intensity, which was due to stirring to some extent improving the Zn^{2+}concentration adsorbed onto the electrode. Despite the increase in stirring intensity, the overall trend was basically the same, which indicates that increasing the stirring rate alone did not change the reaction mechanism. In the studies of other documents [16-19], the influence of stirring speed on zinc ion electrodeposition was not considered.

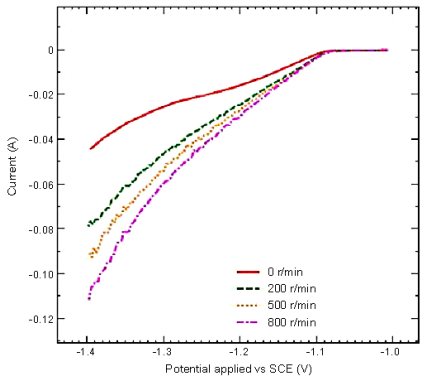

Figure 4a LSV curves of Zn^{2+} reduction on the zinc electrode in zinc (Ⅱ) – NH_4Cl electrolyte at different stirring speeds (the potential range of -1.0V to -1.4V)

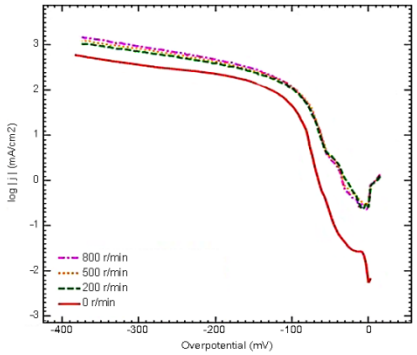

Figure 4b η_k–lg i_K curves of Zn^{2+} reduction on the zinc electrode in zinc (Ⅱ) – NH_4Cl electrolyte at different stirring speeds

3.2.3. Effect of Zn^{2+} concentration

Fig. 5a shows the LSV curves on the zinc electrode in zinc (Ⅱ) – NH_4Cl electrolyte at different Zn^{2+} concentrations. As can be seen from Fig. 5a, at the beginning of the cathodic reaction, the degree of polarization showed obvious differences. This may be because the initial Zn^{2+} concentration was different on the electrode surface when the electrolyte contained different Zn^{2+} concentrations. The Zn^{2+} concentration was higher in the electrolyte, so the initial Zn^{2+} concentration was higher on the electrode surface. It is much easier that Zn^{2+} broke through the film resistance to accept electrons on the high Zn^{2+} concentration electrode surface, and the reaction was relatively fast. This trend was more pronounced at the hybrid control stage. This shows that the higher Zn^{2+} concentration in the electrolyte was more conducive to the Zn^{2+} reduction of cathodic polarization, but the rapid electrode reaction would make the deposited zinc surface loose and uneven.

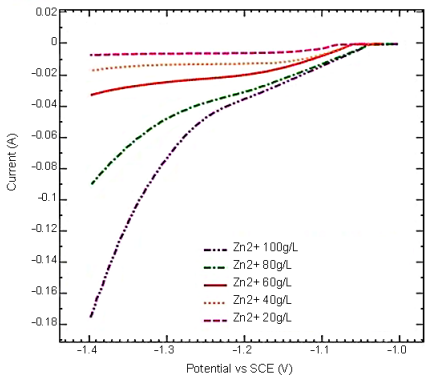

Figure 5a LSV curves of Zn^{2+} reduction on the zinc electrode in zinc (Ⅱ) – NH_4Cl electrolyte at different zinc ion concentrations (the potential range of -1.0V to -1.4V)

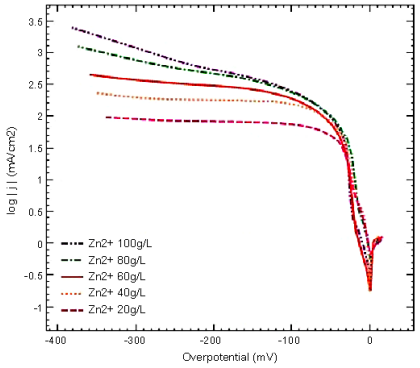

Figure 5b η_k–lg i_K curves of Zn^{2+} reduction on the zinc electrode in zinc (Ⅱ) – NH_4Cl electrolyte at different zinc ion concentrations

Fig. 5b shows the η_k–lgi_K curves on the zinc electrode in zinc (Ⅱ) – NH_4Cl electrolyte at different Zn^{2+} concentrations. From Fig. 5b and equation (2), it can be seen that representation of the linear portion of the curve using the Tafel relationship was undefined, but improving the Zn^{2+} concentration in the electrolyte did not significantly change its exchange current density. Wang [17] has stuided only the influence of different zinc ion concentration on the cell voltage and current efficiency of the zinc electrodeposition process, but the influence mechanism is not studied.

3.2.4. Effect of NH_4^+ concentration

It is known that the stability constants of $Zn(NH_3)_4^{2+}$ and $Zn(Cl)_4^{2-}$ are 2.9×10^9 and 2.3×10^4, which are much greater than the constants of the complex under four-coordination. The stability constant of $Zn(NH_3)_2^{2+}$ is 6.5×10^4, so the form of Zn^{2+} existing in the solution depends on the NH_4^+ concentration and the Cl^- concentration. When $NH_4^+ \geq 40$ g/l, $Zn(NH_3)_m^{2+}$（$m \cong 2$）was the primary form. The form of Zn^{2+} changed from $Zn(NH_3)_2^{2+}$ to $Zn(NH_3)_4^{2+}$ with increasing NH_4^+, which affected the equilibrium electrode potential φ_0 of Zn^{2+} on the zinc electrode, and could also change the pre-conversion course of the electrode reaction.

Fig. 6a shows the LSV curves of Zn^{2+} reduction on the zinc electrode in zinc (Ⅱ) – NH_4Cl electrolyte at different NH_4^+ concentrations. As can be seen from Fig. 6a, the change of LSV curves tended to be gentle with NH_4^+concentration increasing in the electrolyte, and the polarization was more serious. But this polarization may lead to slow Zn^{2+} discharge reduction on the zinc electrode, and make the zinc surface being smoother. Reasons for the polarization of NH_4^+ may be that the coordination number of $Zn(NH_3)_m^{2+}$ increased, the rate of electromigration decreased and the pre-conversion course of the $Zn(NH_3)_m^{2+}$ reduction increased with increasing of NH_4^+concentration.

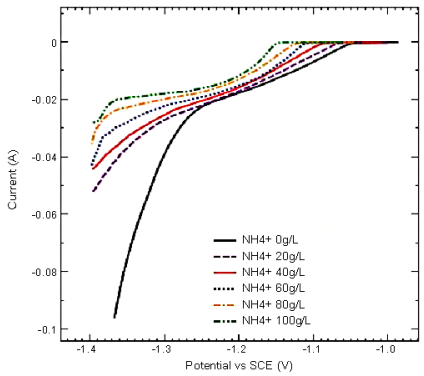

Figure 6a LSV curves of Zn^{2+} reduction on the zinc electrode in zinc (Ⅱ) – NH_4Cl electrolyte at different ammoniumion concentrations (the potential range of -1.0V to -1.4V)

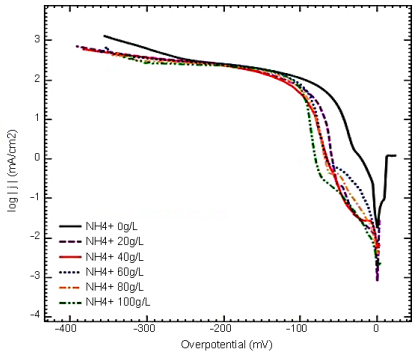

Figure 6b η_k–lg i_K curves of Zn^{2+} reduction on the zinc electrode in zinc (Ⅱ) – NH_4Cl electrolyte at different ammoniumion concentrations

Fig. 6b shows the η_k–lg i_K curves on the zinc electrode in zinc (Ⅱ) – NH_4Cl electrolyte at different NH_4^+ concentrations. As can be seen from Fig. 6b, the curves became very complicated with the change of NH_4^+ concentration in the solution, and this did not accord with the Tafel relationship. This shows that when there was NH_4^+ in the electrolyte, the cathode electrode process was relatively complex, which differed from the conventional electrolysis of the zinc sulfate system. In literature [15], the equilibrium potential, limiting current density and exchange current density of zinc in solutions with different ammonium ion concentrations are studied. Soleimangoli et al. [19] research results showed that adding NH_4Cl could affect the composition and surface morphology of the Ni–Zn coatings. A transition from a Zn-rich Ni–Zn coatings with polyhedral shape to the Ni-rich Ni–Zn coatings with hierarchical nano/mico-conical structure was taken place through adding NH_4Cl as a crystal modifier.

3.3. Study of influence factors on hydrogen evolution reaction

3.3.1. Effect of temperature

Fig. 7a shows the LSV curves of the H^+reduction on the zinc electrode in NH_4Cl electrolyte at different temperatures in no Zn^{2+} solution. It can be seen from Fig. 7a that the H^+reduction reaction could be largely ignored at room temperature, and when the electrolyte temperature $T \geq 313K$, the H^+ reduction reaction became clearer.

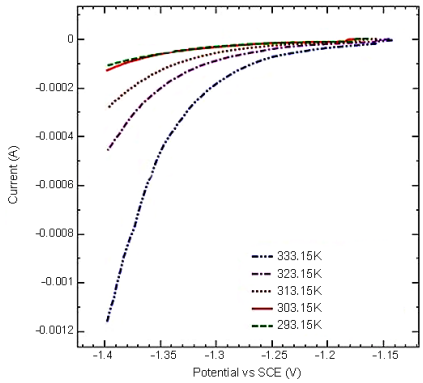

Figure 7a LSV curves of H^+ reduction on the zinc electrode in zinc (Ⅱ) – NH_4Cl electrolyte at different temperatures (the potential range of -1.0V to -1.4V)

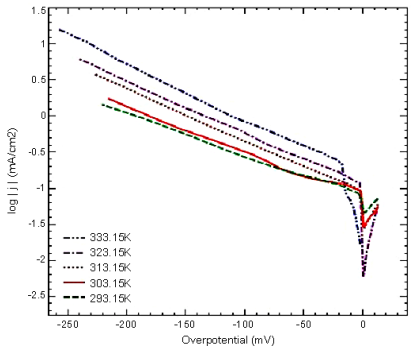

Figure 7b η_k–lg i_K curves of H^+reduction on the zinc electrode in zinc (Ⅱ) – NH_4Cl electrolyte at different temperatures

Fig. 7b shows the η_k–lg i_K curves of the H^+reduction on the zinc electrode in zinc (Ⅱ) – NH_4Cl electrolyte at different temperatures in no Zn^{2+} solution. It is clear that all reactions followed the Tafel relationship. It can be seen that $\alpha n \propto T$ from Fig. 7b and formula (2), and the exchange current densities (i_0) were 5.62×10^{-2} mA/cm^2, 6.31×10^{-2} mA/cm^2, 7.94×10^{-2} mA/cm^2, 1.12×10^{-1} mA/cm^2, and 1.58×10^{-1} mA/cm^2. Successively, αn then became 0.436, 0.451, 0.466, 0.481, and 0.496. This shows that H^+ reduction was a single-electron reaction in the zinc electrode. The standard electrode reaction rate

constant and the discharge rate of the reaction increased with increasing temperature.

3.3.2. Effect of electrode potential

Cell voltage was another important factor which affected the H^+ reduction reaction in the reduction of Zn^{2+}. Therefore, the integral power difference of Zn^{2+} reduction and oxidation was used to investigate whether electrode potential influenced the hydrogen evolution reaction during the zinc deposition process.

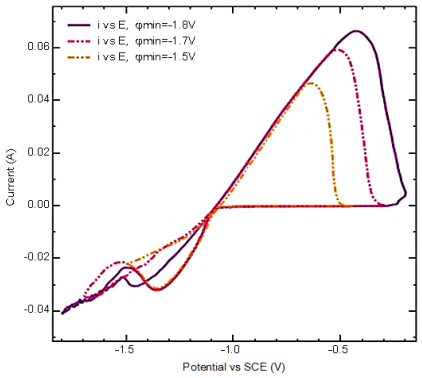

Figure 8a The cycle voltammetry curves H^+ reduction on the gold electrode in zinc (Ⅱ) – NH_4Cl electrolyte at different potential ranges

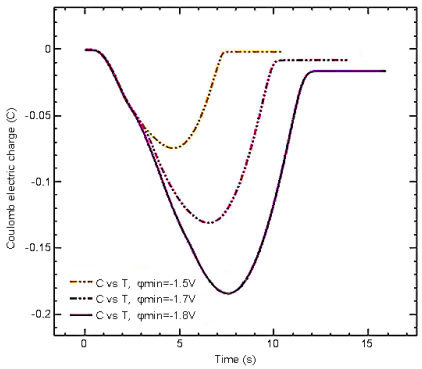

Figure 8b *Q–t* curves H^+ reduction on the gold electrode in zinc (Ⅱ) – NH_4Cl electrolyte at different voltage ranges

Fig. 8a shows the cycle voltammetry curves H^+ reduction on the gold electrode in zinc (Ⅱ) – NH_4Cl electrolyte at different potential ranges. As can be seen from Fig. 8a, with the scanning potential broadening, the curves of cathode reduction late reaction became more unstable. This may be that because the hydrogen evolution reaction was aggravated together with the Zn^{2+} reduction reaction, the Zn^{2+} concentration difference increased, and the migration of ions in the electrolyte was disrupted, then the cathode current produced fluctuation. No other oxidation reaction except for Zn was observed when

the electrode potential was more positive than the OCP, which shows that only the zinc occurred oxidation dissolution reaction in the anodic process.

Fig. 8b shows *Q–t* curves H^+ reduction on the gold electrode in zinc (Ⅱ) – NH_4Cl electrolyte at different voltage ranges. As can be seen from Fig. 8b, the Coulomb electric quantity on both sides of the reduction and oxidation was unsymmetric, which further illustrates that the hydrogen evolution reaction existed in the cathodic process, hydrogen precipitated from the cathodic process could not be oxidized to H^+ in the anodic process at the same potential. The electricity utilization ratio calculated from $\eta^* = (Q_{Me}/Q_T) \times 100\%$ was sequentially 97.90%, 94.06%, and 89.97% under the control potential, which shows that there is high power utilization for zinc electrolysis in a Zn (II)–NH_4Cl system.

Jan et al.[18] studied the influence of the hydrogen evolution on the zinc electrode polarization curves and on the current efficiency of the zinc deposition. It was found that the hydrogen evolution reaction starts to run significantly near the mass transfer limitation of the zinc deposition, since the shape of the zinc electrode polarization curve lacks the plateau of the zinc limiting current density.

4. CONCLUSIONS

1) Cyclic voltammetry investigation shows that Zn^{2+} reduction reactions were irreversible on the gold electrode and the zinc electrode, but the Zn^{2+} reduction rate on the zinc electrode was faster than on the gold electrode. In addition, the Zn^{2+} reduction reaction was a two-electron tandem reaction, and the control step was the first step.

2) The reduction rate of Zn^{2+} increased with an increase in the temperature, stirring intensity and Zn^{2+} concentration, but the effect was not significant when stirring up to a certain magnitude. The form of Zn^{2+} existing in solution related to the NH_4^+ concentration, and increasing the NH_4^+ concentration played a polarization role in the process of Zn^{2+} reduction.

3) Hydrogen evolution increased with an increase of the electrolytic temperature and negative shifting of the cathode potential in the process of Zn^{2+} reduction. Its Tafel constant did not change with temperature. The electron transfer coefficient successively increased with temperature. Q–t curves show that there is high power utilization for zinc electrolysis in a Zn (II)–NH_4Cl system.

ACKNOWLEDGEMENTS
This work was supported by National Natural Science Foundation of China (NO.51304094) and Yunnan Ten Thousand Talents Plan Young & Elite Talents Project（YNWR-QNBJ-2018-327）

References

1. M. Ejtemaei, M. Gharabaghi, M. Irannajad, *Adv. Colloid Interface*, 206(2014)68.
2. X. Ren, Q. Wei, S. Hu, S. Wei, *J. Hazard. Mater.*, 181 (2010) 908.
3. S. H. Ju, M.T. Tang, S.H. Yang, Y.N. Li, *Hydrometallurgy*, 80 (2005) 67.
4. Z. M. Xia, S.H. Yang, M.T. Tang, *RSC Adv.*, 5 (2015) 2663.

5. Y. X. Han, S.B. Ma, Y.B. Wang, *Min. Metall Eng.*, 6 (2014) 56.
6. M. S. Alam, M. Tanaka, K. Koyama, T. Oishi, J.C. Lee, *Hydrometallurgy*, 87 (2007) 36.
7. G. Q. Zheng, L.F. Zheng, H.Z. Cao, *T Nonferr Metal Soc.*, 01 (2005) 165.
8. T. Oishi, K. Koyama, H. Konishi, M. Tanaka, J.C. Lee, *Electrochim. Acta*, 53 (2007) 127.
9. H. J. Zheng, Z.H. Gu, Y.P. Zheng, *Hydrometallurgy*, 90 (2008) 8.
10. S. Rao, T.Z. Yang, D.C. Zhang, *Hydrometallurgy*, 158 (2015) 101.
11. Z. Y. Ding, Z.L. Yin, Q.Y. Chen, *T Nonferr Metal Soc.*, 3 (2013) 832.
12. S. H. Yang, M.T. Tang, Y.F. Chen, *T Nonferr Metal Soc.*, 3 (2004) 626.
13. Z. M. Xia, S.H. Yang, M.T. Tang, *T Nonferr Metal Soc.*, 12 (2013) 3455.
14. H. J. Zheng, Z.H. Gu, J.H. Zhong, *Hydrometallurgy*, 89 (2007) 369.
15. C. Ma, Z.X. Yu, *J. Process. Eng.*, 3 (2003) 68.
16. V. A. Jorge, S.R. Fabiola, L. Isabel, *Electrochim. Acta*, 79 (2012) 109.
16. R. X. Wang, Study on theory and technology for treating low-grade zinc oxide ores to prepare cathode zinc in the Me-NH_4Cl-NH_3-H_2O system, Central South University, (2009) Changsha, China.
17. J. Dundáleka, I. Šnajdra, O. Libánskýa, J. Vránaa, J. Pocedičb, P. Mazúrb and J Koseka, *J. Power Sources*, 372 (2017) 221.
19. F. Soleimangolia, S. A. Hosseinia, A. Davoodib, A. Mokhtaric and M. Alishahia, *Surf. Coat. Tech.*, 394 (2020) 125825.